Improvement of Electrical Performance by Neutron Irradiation Treatment on IGZO Thin Film Transistors

Sera Kwon [1], Jongin Hong [2], Byung-Hyuk Jun [3] and Kwun-Bum Chung [1],*

[1] Division of Physics and Semiconductor Science, Dongguk University, Seoul 04620, Korea;
    serakwon@dongguk.edu
[2] Department of Chemistry, Chung-Ang University, Seoul 06974, Korea; hongj@cau.ac.kr
[3] Advanced Materials Research Division, Korea Atomic Energy Research Institute, Daejeon 34057, Korea;
    bhjun@kaeri.re.kr
* Correspondence: kbchung@dongguk.edu; Tel.: +82-2-2260-3187

Abstract: The effects of the neutron irradiation treatment on indium-gallium-zinc oxide (IGZO) are investigated as a function of the neutron irradiation time. With an increase in neutron irradiation time, the oxygen vacancies associated the oxygen deficient states increase, and both shallow and deep band edge states below the conduction band also increase. Moreover, the conduction band offset continuously decreases because of the increase in the oxygen vacancies with increasing the neutron irradiation time. In IGZO TFTs with the neutron irradiation time for 10 s, superior device performance demonstrates such as the lower threshold voltage, higher field effect mobility, smaller sub-threshold gate swing, larger on-off current ratio, and improved bias stability, comparing those of other IGZO TFTs.

Keywords: neutron irradiation; IGZO; thin-film transistor; electrical performance; electronic structure

1. Introduction

Amorphous oxide semiconductor (AOS) based thin film transistors (TFTs) have attracted attention for next generation electronic devices because AOS TFTs exhibit sufficiently high field effect mobility (>10 cm^2/V·s), capability of uniform deposition over large area, as well as fabrication at room temperature without a defect treatment [1–3]. In the various candidates for the AOS TFTs, indium-gallium-zinc oxide (IGZO) is one of the most promising material. The IGZO is considered suitable inside the TFT backplane that exhibits a high on-current and low off-current, and small subthreshold gate swing, which provides high resolution active matrix organic light emitting diode displays (AMOLEDs) and high frame liquid crystal displays (LCDs) [4,5]. For achieving the higher performance of IGZO based TFTs, a number of studies have been proposed as the treatment methods, including the thermal annealing in various conditions, including ambient atmosphere and pressure [6–8], rapid thermal annealing (RTA) [9], and simultaneous ultraviolet and thermal (SUT) treatment [10]. However, these treatment methods mostly accompany the high temperature, long treatment time, and complication of using vacuum or pressure. To solve these problems, Park et al. [11] and Ahn et al. [12] demonstrated that the hydrogen ion irradiation method improved the electrical characteristics of IGZO based TFTs at room temperature due to the changes of the electronic structures such as the chemical bonding states, band gap, and the band edge states below the conduction band. Despite advantages such as low temperature and a short treatment time, the hydrogen ion irradiation method has critical problems in that hydrogen can diffuse in an oxide matrix as substitutional defect and causes device instability [13–15], therefore, new treatment method to obtain the higher device performance of IGZO based TFTs still has been important issue.

In this paper, we suggest the neutron irradiation treatment method to improve of the electrical characteristics on IGZO based TFTs. In past years, most of the researches have focused on changing the structural properties in several semiconductor materials, because the neutron irradiation induced the structural defects at low temperature [16–18]. From these researches, we believe that the control of neutron irradiation dose can effectively change of the electronic structures by controlling the induced defects in IGZO system without high temperature, long treatment time, and complication of fabrication process. To confirm the effect of neutron irradiation treatment methods, we evaluated the electronic characteristics and electrical performance of IGZO as a function of the neutron irradiation time from 0 to 1000 s.

2. Experiment

For the fabrication of IGZO TFTs, p-type Si substrate was used as the back-gate electrode, and 100-nm-thick SiO_2 layer used as the gate insulator. Further, 50-nm-thick IGZO as the active channel was deposited by radio frequency (RF) sputtering with shadow mask from a sintered In-Ga-Zn-O (1:1:1 at. %) sputtering target. Then, 100-nm-thick ITO as the source/drain electrode was deposited by direct current (DC) sputtering with shadow mask. The fabricated structure of IGZO TFTs schematically illustrates in Figure 1 (a), and the active channel width (W) and length (L) was 800 and 200 um, respectively. After fabrication process, the thermal annealing process carried out at 350 °C for 1 h in ambient air atmosphere. After that, the neutron irradiation process was implemented to IGZO films and IGZO TFTs, it was conducted by using MC-50 cyclotron (Scanditronix, Vislanda, Sweden) at Korea Institute of Radiological and Medical Sciences (KIRAMS), Korea. The neutrons were produced by bombarding protons on a beryllium target with 30 MeV of acceleration energy at 10 uA, then the neutron irradiation dose was approximately 7.0×10^8 ions/cm^2. The neutron irradiation process was performed for 0, 10, 100, and 1000 s under atmospheric pressure at room temperature without a separate chamber.
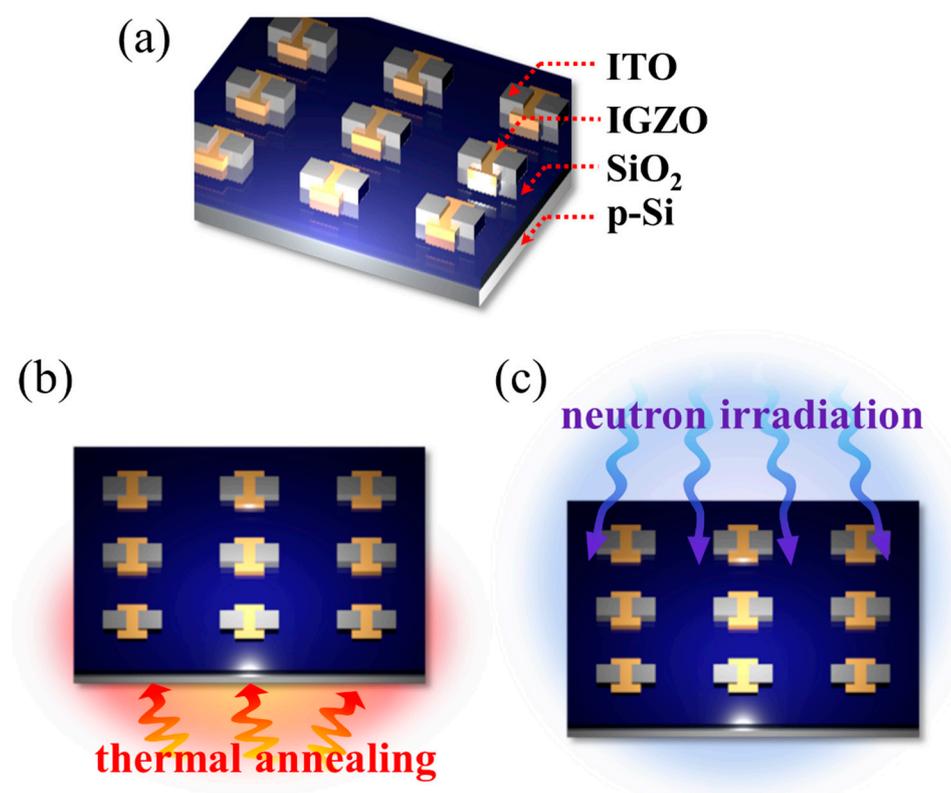
Figure 1. (**a**) Schematic illustration of the structure of IGZO TFTs; (**b**) conventional thermal annealing, and (**c**) the neutron irradiation process.

The thickness of IGZO films was confirmed to approximately 50 nm by using spectroscopic ellipsometry (SE) analysis. X-ray photoelectron spectroscopy (XPS) (Ulvac-phi, Kanagawa, Japan) and SE measured to analysis of the electronic structure associated to the chemical bonding states and band edge states below the conduction band. XPS measurement carried out with monochromatic Al K*a* (*hv* = 1486.7 V) source with a pass energy of 29.35 eV, after Ar ion sputtering with 500 V to eliminate the absorbed OH, C, H_2O, and others on IGZO surface. SE measurement was performed using a rotating-analyzer system with an automatic retarder in the energy range from 1.0 to 5.0 eV at incident angle of 65°. The electrical characteristics of IGZO TFTs were analyzed using a Keithley SCS-4200 (Keithley Instruments, Solon, OH, USA) semiconductor-parameter analyzer.

3. Results and Discussion

Figure 1a shows the schematic structure of IGZO TFTs with bottom gate type. Figure 1b,c schematically illustrates the thermal annealing and neutron irradiation process, respectively. All IGZO films and IGZO TFT samples were implemented the thermal annealing at 350 °C for 1 h in advance of the neutron irradiation treatment, and then imposed the neutron irradiation treatment of 10, 100, and 1000 s in atmospheric pressure at room temperature, whereas IGZO samples with neutron irradiation time for 0 s applied only thermal annealing process.

Figure 2 shows the O 1*s* core-level spectra of IGZO films as a function of the neutron irradiation time from 0 to 1000 s. To analyze specifically the oxygen bonding states, the O 1*s* spectra were normalized and deconvoluted into three Gaussian peaks corresponding to the oxygen species of the metal-oxide bonds of In-O, Ga-O, and Zn-O at 531 ± 0.2 eV (O1), the oxygen species of the oxygen-deficient states at 532 ± 0.2 eV (O2), and the impurity species on the surfaces including chemisorbed or dissociated O_2 or OH at 533 ± 0.2 eV (O3) [19]. The relative area of O1 states decreases from 77.53 to 71.60% with the increase in the neutron irradiation time from 0 to 1000 s, whereas relative area of O2 states gradually increases from 20.01 to 24.62%. These results indicate that the oxygen vacancies associated to the oxygen deficient states of IGZO increase with neutron irradiation time, which contribute to the increase of the carrier concentration due to the generation of additional free electrons as $V_o = V_o^{2+} + 2e^-$ [20]. The relative area of O3 states decreases as increasing the neutron irradiation time to 10 s, while the relative area of O3 rapidly increases as increasing the neutron irradiation time to 1000 s. The increase in O3 states can correlate the degradation of mobility because of charge trapping and scattering [13].
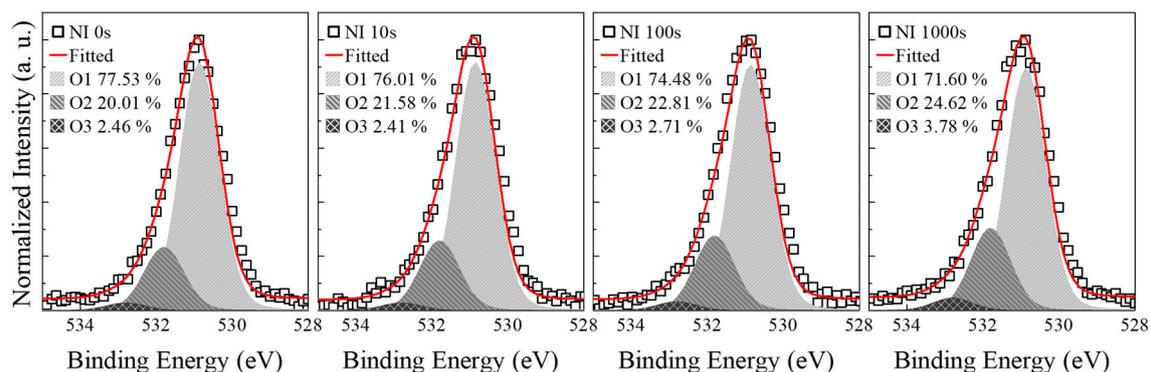
Figure 2. O 1*s* core level spectra deconvoluted with Gaussian fits as a function of the neutron irradiation time.

To understand the optical properties and the electronic structures including the sub-gap states below the conduction band, SE analysis was conducted and the complex refractive index ($\tilde{n} = n+ik$) was obtained as shown in Figure 3a,b. These spectra obtained from simple four-phase model comprising a Si substrate, SiO_2 layer, IGZO over-layer, and an ambient layer [21]. The refractive index *n* associated to the film density slightly decreases with the increase in the neutron irradiation time from 0 to 1000 s, it can be related to the increase of the oxygen vacancies of IGZO films. Figure 3b shows the extinction

coefficient *k* related the absorption properties of IGZO films, and the evolution of the band edge states below the conduction band was found. Then, we performed the quantitative analysis of the band edge states and conduction band with a Gaussian function (band edge states) and a Tauc-Lorentz function (conduction band states), as shown in Figure 3c [12]. The Gaussian fits compose to shallow band edge state (D1) and deep band edge state (D2), which are related to the oxygen deficient bonding states. The band edge states strongly correlated to the electrical characteristics including carrier concentration and mobility, depending on the relative position within bandgap. The relative area of D1 slightly increases, whereas that of D2 rapidly increases as a function of the neutron irradiation time. The increase in D1 associates the enhancement of the carrier concentration, while the increase in D2 affects to degradation of mobility due to charge trapping and scattering during the carrier transport [16]. From the above interpretations, we confirm that the changes of the band edge states associated to the oxygen vacancies strongly affect the modulation of the electrical characteristics.
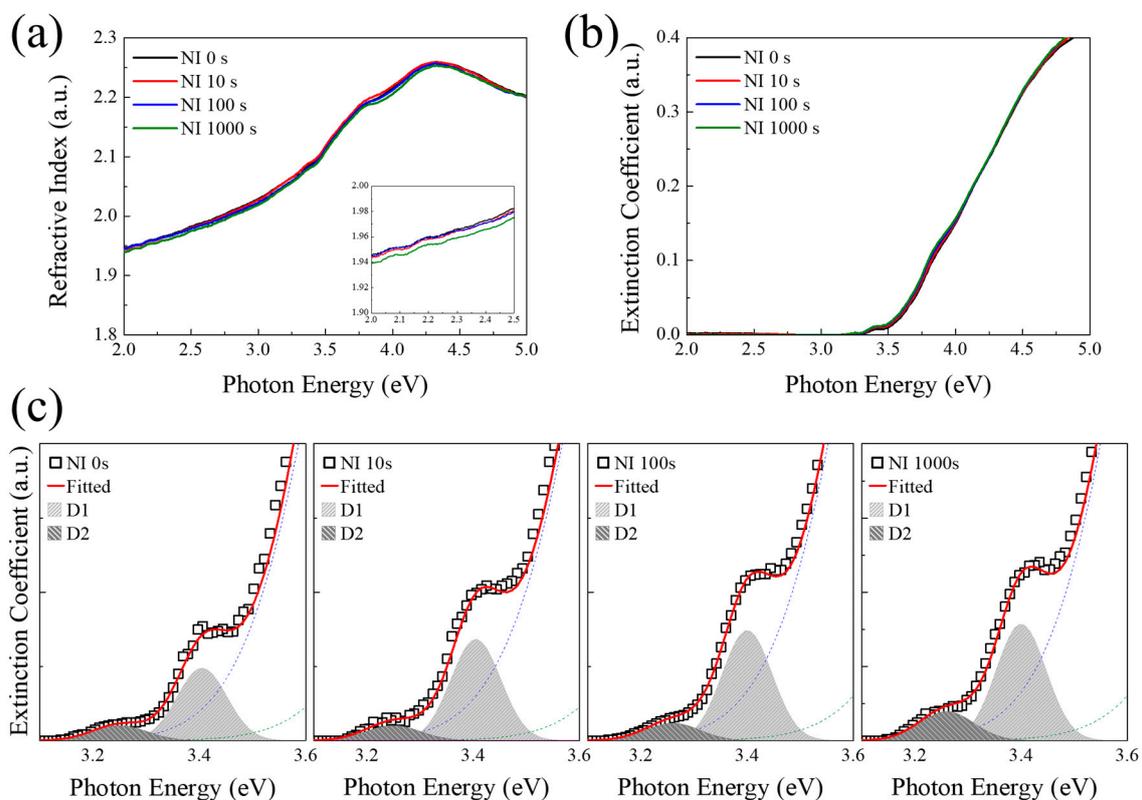
Figure 3. (**a**) Refractive index *n*; (**b**) extinction coefficient *k* extracted using SE analysis, and (**c**) the evolution of the relative defect absorption areas below the conduction band of IGZO films for two distinct band edge states (D1 and D2), calculated by the deconvoluted Gaussian function fitting.

Figure 4a shows the valence band region using XPS measurement, the linear extrapolation was also used to obtain the valence band offset using the energy difference between the valence band maximum and Fermi level (valence band offset, ΔE_{VB}). Figure 4b shows the results of the optical band gap which is obtained from the linear extrapolation based on the point at which the extinction coefficient increases. Using the values of the valence band offset and band gap, the energy band alignment can be schematically illustrated as shown in Figure 3c, as a function of the neutron irradiation time. The relative energy difference between Fermi level and the conduction band minimum (conduction band offset, ΔE_{CB}) is clearly observed. The conduction band offset is smaller from 0.34 to 0.13 eV with increasing the neutron irradiation time from 0 to 1000 s, respectively, which generally means a higher carrier concentration and interstitial atoms in channel layer as a function of the neutron irradiation time [10]. This trend strongly relates with the evolution of shallow band edge states below

the conduction band edge in shown in Figure 3c. From the above results, we believe that the changes of the electronic structures including the chemical bonding states, band edge states below the conduction band, and energy band structures of IGZO films can be ascribed to the electrical performance of IGZO based TFTs.
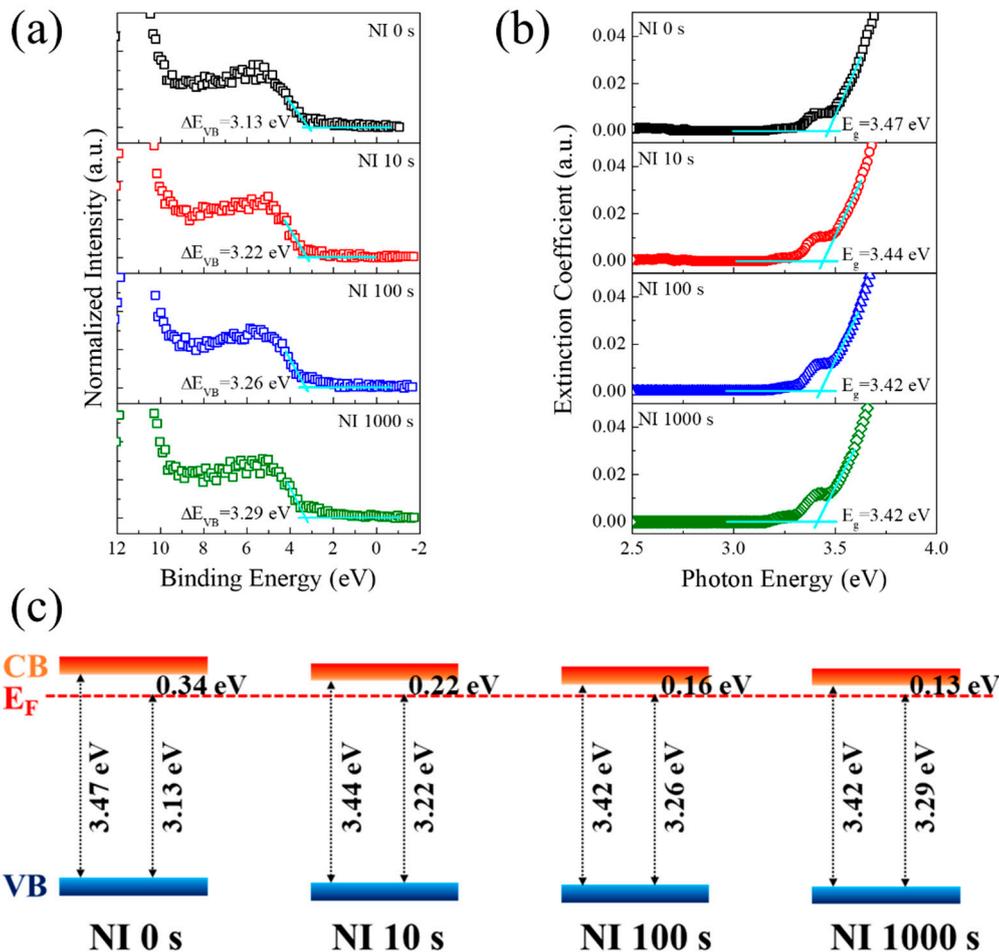
Figure 4. (**a**) Valence band offset (ΔE_{VB}) from valence band spectra; (**b**) optical band gap (E_g) from extinction coefficient, and (**c**) the schematic energy band alignment of IGZO films as a function of the neutron irradiation time, including the relative energy position of Fermi level (E_F) with respect to the conduction band minimum and the valence band maximum.

Figure 5a shows the transfer characteristics of IGZO TFTs as a function of the neutron irradiation time. During the measurement of drain current (I_D), drain voltage (V_D) was fixed at 10 V and gate voltage (V_G) swept from –20 to 30 V. The parameters including field effect mobility in saturation (μ_{sat}) and linear region (μ_{lin}), threshold voltage (V_{th}), subthreshold gate swing (S.S), and on-off current ratio (I_{ON}/I_{OFF}) describe the performance of TFTs, which as derived from the I-V transfer curves. The μ_{sat} and μ_{lin} are calculated from saturation region and linear region according to Equations (1) and (2) [22]:

$$\mu_{sat} = \frac{\partial I_D}{\partial V_G} \frac{L}{WC_{ox}(V_G - V_{th})} \tag{1}$$

$$\mu_{lin} = \frac{\partial I_D}{\partial V_G} \frac{L}{WC_{ox}V_D} \tag{2}$$

where, L is channel length, W is width, and C_{ox} is the gate capacitance per unit area of the gate oxide. The V_{th} is calculated by fitting a straight line to the plot of the square root of I_D versus V_G in the saturation region.

In addition, the S.S was extracted by Equation (3) [9]

$$S.S = \frac{\partial V_G}{\partial \log I_D} \tag{3}$$

The I_{ON}/I_{OFF} is the quantitative amount representing the switching efficiency of TFT, which describes the ratio of the largest current to the lowest current. The extracted electrical parameters are summarized in Table 1. The IGZO TFTs with the neutron irradiation time for 0 s (only thermal annealing at 350 °C) have V_{th} of 2.55 V, S.S of 0.53 V/decade, μ_{sat} of 8.84 cm^2/V·s, and μ_{lin} of 5.11 cm^2/V·s. As increasing the neutron irradiation time to 10 s, V_{th} slightly shifts to negative voltage (2.04 V) and on-current changes to higher, then the value of μ_{sat} (10.60 cm^2/V·s), μ_{lin} (10.39 cm^2/V·s), I_{ON}/I_{OFF} (1.78 × 10^6) and S.S (0.36 V/decade) improve than those of IGZO TFTs with the neutron irradiation time for 0 s. The better performance of the neutron irradiation time for 10 s can be explained that the changes of the electronic structures such as the increase of shallow band edge states and reduced conduction band offset caused by the increase of the oxygen deficient states. Increasing the neutron irradiation time to 100 s and 1000 s, V_{th} continuously shifts to negative voltages, while on-currents fall than that of IGZO TFTs with the neutron irradiation time for 10 s. It is correlated that the oxygen vacancies in shallow band edge states can induce the carrier concentration and threshold voltage negatively shifts, while the oxygen vacancies in deep band edge states lead to degradation of carrier transport due to the increase of charge trapping and scattering.
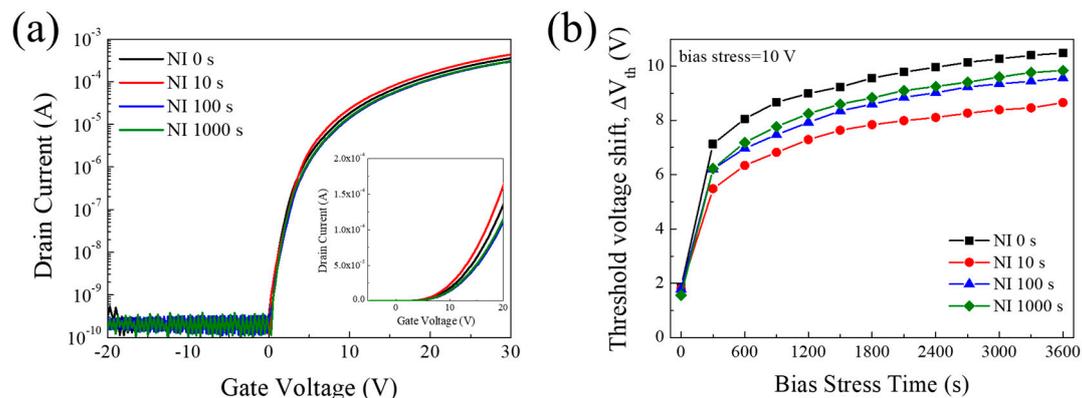
Figure 5. (**a**) Transfer curves (inset shows the linear scales) and (**b**) shift of threshold voltage under positive bias stress of IGZO TFTs as a function of the neutron irradiation time.

Table 1. The electrical characteristics of IGZO TFTs as a function of the neutron irradiation time.

Neutron Irradiation Time (s)	μ_{sat} (cm^2/V·s)	μ_{lin} (cm^2/V·s)	V_{th} (V)	S.S (V/decade)	I_{ON}/I_{OFF}
0	8.84 ± 0.88	5.11 ± 0.51	2.55 ± 0.38	0.53 ± 0.05	9.68 × 10^5 ± 4.84 × 10^4
10	10.60 ± 0.53	10.39 ± 0.73	2.04 ± 0.20	0.36 ± 0.04	1.78 × 10^6 ± 8.90 × 10^4
100	7.98 ± 0.56	5.50 ± 0.55	2.02 ± 0.20	0.61 ± 0.06	1.25 × 10^6 ± 6.25 × 10^4
1000	7.69 ± 0.77	4.22 ± 0.42	1.84 ± 0.18	0.67 ± 0.07	1.23 × 10^6 ± 6.15 × 10^4

Figure 5b shows the bias stability of IGZO TFTs as a function of the neutron irradiation time under positive bias stress (PBS) of 10 V for 3600 s at the atmosphere. V_{th} value continuously shifts toward

the positive voltage as increasing the stress time in all IGZO TFTs, it is related that absorbed oxygen species from the atmosphere can capture electrons in IGZO channel layer and generate the negatively charged species under PBS by $O_2 + e^- = O_2^-$ [23]. In IGZO TFTs with the neutron irradiation time for 0 s (only thermal annealing at 350 °C), the V_{th} shifts toward positive voltage region to 10.50 V, it is the largest variation of V_{th} among the IGZO TFTs as a function of the neutron irradiation time. As the increase of the neutron irradiation time for 10, 100, and 1000 s, the V_{th} shifts toward positive voltage of 8.66, 9.55, and 9.85 V, respectively. From this result of bias stability, the neutron irradiation method affects to the device stability to reduce the trapping of electrons at the atmosphere under PBS. From these results, the electronic structures such as the chemical bonding states, feature of conduction band, the band edge states below the conduction band, and the band structures contribute to changes of the carrier concentration and mobility of IGZO, and lead to the modification of the device performance of IGZO TFTs. Moreover, these results suggest that the neutron irradiation process can be promising method for manipulating IGZO based TFTs.

4. Conclusions

In conclusion, the influence of the neutron irradiation process on the electronic structure of IGZO films and electrical characteristics of IGZO TFTs has been performed as a function of the neutron irradiation time. The oxygen species of the metal-oxide bonds slightly decrease, while the oxygen species of the oxygen deficient states and impurity species increase in the increase the neutron irradiation time. The refractive index related to the film density decreases due to the increase of the oxygen vacancies in IGZO films, and the band edge states below the conduction band increase as a function of the neutron irradiation time. In the band edge states below the conduction band, the shallow band edge states slightly increase, whereas the deep band edge states rapidly increase. The conduction band offset continuously decreases with the increase in the neutron irradiation time, these trends are expected to contribution of the modulation of the electrical characteristics. The electrical characteristics of IGZO TFT with the neutron irradiation time for 10 s has better performance, such as the relatively lower threshold voltage of 2.04 V, higher field effect mobility of 10.60 cm^2/V·s and 10.39 cm^2/V·s in saturation and linear region, respectively, smaller sub threshold gate swing of 0.36 V/decade, and larger on-off current ratio of 1.78×10^6, than those of others. Further, the device stability also improves under positive bias stress. From this research, it is expected that the neutron irradiation process is useful method for manipulating oxide based TFT at room temperature, and in a very short time of a few seconds.

Author Contributions: Conceptualization, J.H., B.-H.J. and K.-B.C.; formal analysis, S.K.; investigation, S.K.; data curation, K.-B.C.; writing—original draft preparation, S.K.; writing—review and editing, S.K., K.-B.C.; supervision, K.-B.C. All authors have read and agreed to the published version of the manuscript.

Funding: This research was funded by the National Research Foundation Grant (NRF-2013M2A8A1035822, 2017M2A8A1066683) from Ministry of Science, ICT and Future Planning (MSIP) of Republic of Korea. The authors express their sincere thanks to the staff of the MC-50 Cyclotron Laboratory (KIRAMS), for the excellent operation and their support during the experiment.

Conflicts of Interest: The authors declare no conflict of interest.

References

1. Nomura, K.; Ohta, H.; Takagi, A.; Kamiya, T.; Hirano, M.; Hosono, H. Room-temperature fabrication of transparent flexible thin-film transistors using amorphous oxide semiconductors. *Nature* **2004**, *432*, 488–492. [CrossRef] [PubMed]

2. Takagi, A.; Nomura, K.; Ohta, H.; Yanagi, H.; Kamiya, T.; Hirano, M.; Hosono, H. Carrier transport and electronic structure in amorphous oxide semiconductor. *Thin Solid Films* **2005**, *486*, 38–41. [CrossRef]

3. Kim, M.; Jeong, J.H.; Lee, H.J.; Ahn, T.K.; Shin, H.S.; Park, J.-S.; Jeong, J.K.; Mo, Y.-G.; Kim, H.D. High mobility bottom gate InGaZnO thin film transistor with SiO$_x$ etch stopper. *Appl. Phys. Lett.* **2007**, *90*, 212114. [CrossRef]

4. Yabuta, H.; Sano, M.; Abe, K.; Aiba, T.; Den, T.; Kumomi, H.; Nomura, K.; Hosono, H. High-mobility thin-film transistor with amorphous InGaZnO$_4$ channel fabricated by room temperature rf-magnetron sputtering. *Appl. Phys. Lett.* **2006**, *89*, 112123. [CrossRef]

5. Lin, C.-L.; Chang, W.-Y.; Hung, C.-C. Compensating pixel circuit driving AMOLED display with a-IGZO TFTs. *IEEE Electron. Dev. Lett.* **2013**, *34*, 1166–1168. [CrossRef]

6. Nomura, K.; Kamiya, T.; Hirano, M.; Hosono, H. Origins of threshold voltage shifts in room-temperature deposited and annealed a-In-Ga-Zn-O thin-film transistors. *Appl. Phys. Lett.* **2009**, *95*, 013502. [CrossRef]

7. Kikuchi, Y.; Nomura, K.; Yanagi, H.; Kamiya, T.; Hirano, M.; Hosono, H. Device characteristics improvement of a-In-Ga-Zn-O TFTs by low-temperature annealing. *Thin Solid Films* **2010**, *518*, 3017–3021. [CrossRef]

8. Ji, K.H.; Kim, J.-I.; Jung, H.Y.; Park, S.Y.; Choi, R.; Kim, U.K.; Hwang, C.S.; Lee, D.; Hwang, H.; Jeong, J.K. Effect of high-pressure oxygen annealing on negative bias illumination stress-induced instability of InGaZnO thin film transistors. *Appl. Phys. Lett.* **2011**, *98*, 103509. [CrossRef]

9. Wu, H.-C.; Chien, C.-H. High performance InGaZnO thin film transistor with InGaZnO source and drain electrodes. *Appl. Phys. Lett.* **2013**, *102*, 062103. [CrossRef]

10. Tak, Y.J.; Yoon, D.H.; Yoon, S.; Choi, U.H.; Sabri, M.M.; Ahn, B.; Kim, H.J. Enhanced electrical characteristics and stability via simultaneous ultraviolet and thermal treatment of passivated amorphous In-Ga-Zn-O thin-film transistors. *ACS Appl. Mater. Interfaces* **2014**, *6*, 6399–6405. [CrossRef]

11. Park, H.-W.; Choi, M.-J.; Jo, Y.C.; Chung, K.-B. Low temperature processed InGaZnO thin film transistor using the combination of hydrogen irradiation and annealing. *Appl. Surf. Sci.* **2014**, *321*, 520–524. [CrossRef]

12. Ahn, B.D.; Park, J.-S.; Chung, K.B. Facile fabrication of high-performance InGaZnO thin film transistor using hydrogen ion irradiation at room temperature. *Appl. Phys. Lett.* **2014**, *105*, 163505. [CrossRef]

13. Noh, H.-K.; Chang, K.J.; Ryu, B.; Lee, W.-J. Electronic structure of oxygen-vacancy defects in amorphous In-Ga-Zn-O semiconductors. *Phys. Rev. B* **2011**, *84*, 115205. [CrossRef]

14. Li, H.; Guo, Y.; Robertson, J. Hydrogen and the light-induced bias instability mechanism in amorphous oxide semiconductors. *Sci. Rep.* **2017**, *7*, 16858. [CrossRef] [PubMed]

15. Kwak, S.-M.; Kim, H.-R.; Jang, H.-W.; Yang, J.-H.; Mamoru, F.; Yoon, S.-M. Improvement in bias-stress and long-term stabilities for In-Ga-Zn-O thin-film transistors using solution-process-compatible polymeric gate insulator. *Org. Electron.* **2019**, *71*, 7–13. [CrossRef]

16. Snead, L.L.; Zinkle, S.J.; Hay, J.C.; Osborne, M.C. Amorphization of SiC under ion and neutron irradiation. *Nucl. Instrum. Methods Phys. Res. B* **1998**, *141*, 123–132. [CrossRef]

17. Bates, J.B.; Hendricks, R.W.; Shaffer, L.B. Neutron irradiation effects and structure of noncrystalline SiO$_2$. *J. Chem. Phys.* **1974**, *61*, 4163–4176. [CrossRef]

18. Yano, T.; Ichikawa, K.; Akiyoshi, M.; Tachi, Y. Neutron irradiation damage in aluminum oxide and nitride ceramics up to a fluence of 4.2×10^{26} n/m^2. *J. Nuclear Mater.* **2000**, *283–287*, 947–951. [CrossRef]

19. Ishida, T.; Kobayashi, H.; Nakako, Y. Structures and properties of electron-beam-evaporated indium tin oxide films as studied by x-ray photoelectron spectroscopy and work-function measurements. *J. Appl. Phys.* **1993**, *73*, 4344–4350. [CrossRef]

20. Walsh, A. Surface oxygen vacancy origin of electron accumulation in indium oxide. *Appl. Phys. Lett.* **2011**, *98*, 261910. [CrossRef]

21. Chung, K.-B.; Seo, H.; Long, J.P.; Lucovsky, G. Suppression of defect states in HfSiON gate dielectric films on n-type Ge(100) substrates. *Appl. Phys. Lett.* **2008**, *93*, 182903. [CrossRef]

22. Cai, J.; Han, D.; Geng, Y.; Wang, W.; Wang, L.; Zhang, S.; Wang, Y. High-performance transparent AZO TFTs fabricated on glass substrate. *IEEE Transac. Electron. Dev.* **2013**, *60*, 2432–2435. [CrossRef]

23. Fuh, C.-S.; Liu, P.-T.; Chou, Y.-T.; Teng, L.-F.; Sze, S.M. Role of oxygen in amorphous In-Ga-Zn-O thin film transistor for ambient stability. *ECS J. Solid State Sci. Technol.* **2013**, *2*, Q1–Q5. [CrossRef]